UC Riverside

UC Riverside Previously Published Works

Title

Extending supramolecular fullerene-porphyrin chemistry to pillared metal-organic frameworks

Permalink

https://escholarship.org/uc/item/6bg7651p

Journal

Proceedings of the National Academy of Sciences of the United States of America, 99(8)

ISSN

0027-8424

Authors

Sun, Dayong
Tham, Fook S
Reed, Christopher A
et al.

Publication Date

2002-04-16

DOI

10.1073/pnas.072602399

Peer reviewed

eScholarship.org Powered by the California Digital Library
University of California

Extending supramolecular fullerene-porphyrin chemistry to pillared metal-organic frameworks

Dayong Sun*, Fook S. Tham*, Christopher A. Reed*†, and Peter D. W. Boyd†‡

*Department of Chemistry, University of California, Riverside, CA 92521-0403; and ‡University of Auckland, Private Bag, Auckland, New Zealand

Edited by Jack Halpern, University of Chicago, Chicago, IL, and approved February 6, 2002 (received for review November 9, 2001)

Porphyrins and fullerenes are spontaneously attracted to each other. This supramolecular recognition element can be exploited to produce ordered arrays of interleaved porphyrins and fullerenes. C_{60}·H_2TpyP·$Pb(NO_3)_2$·1.5TCE (H_2TpyP = tetra-4-pyridylporphyrin; TCE = 1,1,2,2-tetrachloroethane) crystallizes in the tetragonal *P*4/*n* space group and the structure has been solved to high resolution. The Pb^{2+} ions connect the pyridylporphyrins in infinite sheets with an interlayer spacing of 12.1 Å. The fullerenes are intercalated between these layers, acting as pillars. The 6:6 ring juncture bonds of C_{60} are centered over the porphyrins, bringing the layers into strict tetragonal register. This arranagement identifies the fullerene–porphyrin interaction as a structure-defining element. The same motif is seen in a related ribbon structure having C_{70} intercalated into HgI_2-linked H_2TpyTP. The supramolecular design principles involved in assembling these chromophores may have applications in materials science.

A major theme of contemporary chemistry is the identification and manipulation of the weak forces that dictate crystal structures (1–6). Such ''crystal engineering'' promises to shift our understanding of the formation of solid-state structures from a process of empirical self-assembly to a rational consideration of component shape, the summation of weak intermolecular forces, and the dynamics of crystal growth. Thus, the shapes of molecules, their supramolecular recognition elements, and crystal growth conditions are the manipulable variables. Solution-phase supramolecular chemistry is inextricably connected to crystal growth and packing. These fields inform each other and precedent for one can typically be found in the other.

The shape propagation possibilities of tetraphenylporphyrins (7, 8) were successfully fused with supramolecular assembly principles by Robson and co-workers in the early 1990s to create novel, highly porous frameworks containing many solvent molecules. The potential of these fragile structures to act like zeolites in separations and catalysis has stimulated intense activity in the synthesis of more robust systems (9–17), using labile coordinate bonds or H-bonding as the supramolecular recognition elements (18–22).

In this paper we report the use of another supramolecular recognition element to manipulate the structures of extended porphyrin systems. It involves the attraction of a fullerene to the center of a porphyrin. The unexpectedly close approach of a curved π surface to the center of a flat π surface was originally recognized in the x-ray crystal structure of a fullerene–porphyrin conjugate (23). Subsequent cocrystallization studies of fullerenes with porphyrins (or metalloporphyrins) established the generality of the phenomenon (24, 25), and discrete complexes of fullerenes in bisporphyrin (26) or ''jaws porphyrin'' hosts (27, 28) have illustrated the supramolecular chemistry principles involved. The interaction is primarily van der Waals in nature (24) but is influenced by a summation of other weak forces. These include electrostatics, coordinate bond formation, charge transfer, and solvation effects (28). Notably, the traditional paradigm of supramolecular chemistry is not followed. There is no necessity to match a concave host with a convex guest.

The tetragonal shapes of porphyrins and the globular shapes of fullerenes make them attractive candidates for assembling supramolecular structures. We wondered whether fullerenes could act as pillars and organizing elements in layered porphyrinic structures. Fullerene pillars might strengthen porous porphyrin frameworks, giving them greater potential as ''organic zeolites.'' There are other potential applications as light-harvesting devices (29–31), molecular conductors, or magnets (32–34).

One of the most versatile components for constructing porphyrin frameworks is tetra-4-pyridylporphyrin (H_2TpyP).

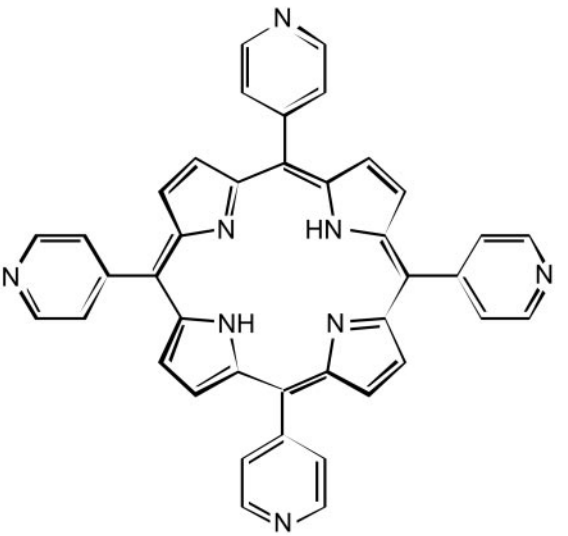

The tetragonal orientation of the peripheral pyridine ligands allows infinite parallel sheet or ribbon structures to form when the *p*-pyridyl groups are linked together by labile metal ions. When crystals of these materials are grown in the presence of fullerenes, intercalation occurs in the solvent space between the porphyrin layers.

Materials and Methods

H_2TpyP was purchased from Aldrich, and C_{60} and C_{70} were from MER (Tucson, AZ).

H_2TpyP·$Pb(NO_3)_2$·C_{60}·1.5TCE, 1. A methanol solution of $Pb(NO_3)_2$ was carefully layered on a 1,1,2,2-tetrachloroethane (TCE) solution of C_{60} and H_2TpyP. Crystals grew over several weeks along with starting materials. A black prism ($0.10 \times 0.14 \times 0.23$ mm^3) was selected from the mixture of crystals for single-

This paper was submitted directly (Track II) to the PNAS office.

Abbreviations: H_2TpyP, tetra-4-pyridylporphyrin; TCE, 1,1,2,2-tetrachloroethane; SEM-EDX, energy-dispersive x-ray techniques under scanning electron microscopy conditions.

†To whom reprint requests may be addressed. E-mail: chris.reed@ucr.edu or pdw.boyd@auckland.ac.nz.

 www.pnas.org/cgi/doi/10.1073/pnas.072602399

crystal x-ray diffraction (identification number ucr38t4n, $C_{112}H_{36}Cl_{24}N_{10}O_6Pb$). The elemental composition deduced from the single-crystal data were consistent with elemental analysis based on energy-dispersive x-ray techniques (microprobe analysis) on individual crystals under scanning electron microscopy conditions (SEM-EDX). The crystal was mounted on a glass fiber and coated with epoxy resin to prevent loss of lattice solvent. X-ray intensity data were collected at 213(2) K on a Bruker SMART 1000 (35) platform–charge-coupled device (CCD) x-ray diffractometer system (Mo radiation, $\lambda = 0.71073$ Å, 50-kV/45-mA power). The CCD detector was placed 3.4310 cm from the crystal. A total of 1,926 frames were collected for a hemisphere of reflections (scan width of 0.3° in ω; ϕ angles of 0°, 90°, 180°, and 0° for every 1,212, 435, 230, and 50 frames, respectively, 120 sec per frame exposure time). The frames were integrated by using the Bruker SAINTPLUS software package (36) with a narrow-frame integration algorithm. Based on a tetragonal crystal system, the integrated frames yielded a total of 52,949 reflections at a maximum 2θ angle of 52.84° (0.80-Å resolution), of which 5,286 were independent reflections ($R_{int} = 0.1201$, $R_{sig} = 0.0645$, redundancy = 10.0, completeness = 99.8%), and 3,217 (60.9%) reflections were greater than $2\sigma(I)$. The unit cell parameters were $a = 20.6507(18)$ Å, $b = 20.6507(18)$ Å, $c = 12.0714(17)$ Å, $\alpha = 90°$, $\beta = 90°$, $\gamma = 90°$, $V = 5147.9(10)$ Å^3, $Z = 2$, calculated density $D_c = 1.726$ g/cm^3. Absorption corrections were applied (absorption coefficient $\theta = 2.326$ mm^{-1}) to the raw intensity data by using the SADABS program in the SAINTPLUS software. The Bruker SHELXTL (Version 5.1) software package (37) was used for phase determination and structure refinement. The distribution of intensities ($E^2 - 1 = 0.923$) and systematic absent reflections indicated two possible space groups, $P4/n$ and $P4/nmm$. The space group $P4/n$ was later determined to be correct. Direct methods of phase determination followed by two Fourier cycles of refinement led to an electron density map from which most of the non-hydrogen atoms were identified in the asymmetry unit of the unit cell. With subsequent isotropic refinement all of the non-hydrogen atoms were identified. The structure was refined as a tetragonal merohedral twin (twin law 0 1 0 1 0 0 0 0 −1). The C_{60} and the porphyrin were located on a fourfold rotation axis parallel to the c-axis. The C_{60} was modeled as a disordered C_{60} by using restraints where each C_{60} site was 25% occupied. Besides the fourfold rotation symmetry, each pyridyl ring was modeled as 50% disorder. The $Pb(NO_3)_2$ was located on a fourfold inversion axis parallel to the c-axis. There were five partially occupied TCE solvent molecules in the asymmetry unit and they all added up to 1.5 TCE molecules. Atomic coordinates and isotropic and anisotropic displacement parameters of all of the non-hydrogen atoms were refined by means of a full matrix least-squares procedure on F^2. All hydrogen atoms were included in the refinement in calculated positions riding on the atoms to which they were attached. The refinement converged at $R1 = 0.0454$, $wR2 = 0.1108$, with $I > 2\sigma(I)$. The largest peak and hole in the final difference map were 1.166 and −1.482 e/Å^3.

$Pb(NO_3)_2$·H_2TpyP·C_{70}·*x*Solvent, 2. Black cubes were grown over 1 month by layered diffusion of saturated $Pb(NO_3)_2$ in methanol and 1:1 H_2TpyP and C_{70} in TCE. Space group $P4/n$, $a = 20.780(2)$ Å, $b = 20.780(2)$ Å, $c = 12.491(2)$ Å, $\alpha = 90°$, $\beta = 90°$, $\gamma = 90°$, $V = 5394(2)$ Å^3, $Z = 2$, $2\theta = 52.74°$ (0.80-Å resolution). Preliminary structure solution from 43,625 reflections at a maximum 2θ angle of 52.74° (0.80-Å resolution), of which 5,523 were independent reflections and 3,993 (72.3%) reflections were $>2\sigma(I)$, led to $R_{int} = 0.0534$, $R_{sig} = 0.0359$. With the anisotropic refinement of the Pb atom and isotropic refinement of the rest of the atoms, the refinement converged to $R1 = 0.1786$.

HgI_2·H_2TpyP·C_{70}·*x*Solvent, 3. Thin brown-black plates were grown by layered diffusion of HgI_2 in methanol and 1:1 H_2TpyP and C_{70} in TCE. A fragment of a prism ($0.13 \times 0.07 \times 0.02$ mm^3) was used for the single-crystal x-ray diffraction study of ucr42r1s ($C_{40}H_{24}N_4HgI_2C_{70}$). Data were collected at 213(2) K in a manner similar to that for **1** with the detector 3.41 cm from the crystal. Based on a monoclinic-P crystal system, the integrated frames yielded a total of 15,427 reflections at a maximum 2θ angle of 49.42° (0.85-Å resolution), of which 6,505 were independent reflections ($R_{int} = 0.0805$, $R_{sig} = 0.0879$, redundancy = 2.4, completeness = 99.8%) and 4,562 (70.1%) reflections were greater than $2\sigma(I)$. The unit cell parameters were $a = 12.500(6)$ Å, $b = 13.627(6)$ Å, $c = 12.614(6)$ Å, $\alpha = 90°$, $\beta = 119.680°$, $\gamma = 90°$, $V = 1866.9(15)$ Å^3, $Z = 2$, and $D_c = 2.105$ g/cm^3. Absorption corrections were applied (absorption coefficient $\mu = 5.826$ mm^{-1}) to the raw intensity data. The maximum/minimum transmission factors were 0.8924/0.5180. The distribution of intensities ($E^2 - 1 = 0.850$) and systematic absent reflections indicated three possible space groups, $P2$, $P2/m$, on Pm. The most probable space group was Pm. The Patterson method was used to locate the Hg and two I atoms. Direct methods of phase determination followed by two Fourier cycles of refinement led to an electron density map from which most of the non-hydrogen atoms were identified in the asymmetry unit. With subsequent isotropic refinement, all of the non-hydrogen atoms were identified. Half a molecule of $C_{40}H_{24}N_4HgI_2C_{70}$ was present in the asymmetry unit. A rigid-body model with restraints was used to model the structure. The C_{70} and $C_{40}H_{24}N_4HgI_2$ were located on the mirror plane. The space group Pm was selected over $P2$, $P2/m$, $C2$, $C2/m$, and Cm because the refinement process using the other space groups was unstable and C_{70} did not fit as well in the special position of these space groups. Attempts were made to refine the structure as orthorhombic space groups $C222$, $Cmmm$, and $Cmm2$. It was not possible to fit the C_{70} in the special position of these space groups. The structure was refined as a racemic twin with unequal components (major and minor components were 55% and 45%, respectively). Solvent molecules (methanol, TCE) were not identified or refined because high thermal parameters indicated severe disorder and SEM-EDX analysis gave variable results regarding precise composition. Atomic coordinates and isotropic and anisotropic displacement parameters of all of the non-hydrogen atoms were refined by means of a full matrix least-squares procedure on F^2. All of the hydrogen atoms were included in the refinement in calculated positions riding on the atoms to which they were attached. The refinement converged at $R1 = 0.0775$, $wR2 = 0.2052$, with intensity $I > 2\sigma(I)$. The largest peak and hole in the final difference map were 5.727 and −3.029 e/Å^3.

Supporting Information. X-ray data sets for compounds **1**, **2**, and **3** are published as supporting information on the PNAS web site, www.pnas.org.

Results and Discussion

Fullerene-Pillared Sheets. When H_2TpyP, $Pb(NO_3)_2$, and C_{60} are mixed in a layered TCE solution, crystals of C_{60}·H_2TpyP·$Pb(NO_3)_2$·1.5TCE, **1**, form spontaneously. Solving the x-ray structure was a crystallographic tour de force, requiring problems of merohedral twinning, disorder in the fullerene, and partial solvent occupancy to be overcome in an incommensurate structure.

As shown in Fig. 1, the porphyrins in **1** are tetragonally connected by Pb^{2+} ions in an infinite two-dimensional sheet structure. Nitrate anions are axially coordinated above and below the Pb^{2+} ions. This motif is the same as that found in the corresponding non-fullerene Pb(II) dihalide system (15).

As illustrated in Fig. 2, the fullerenes are sandwiched between these porphyrinic layers. The interlayer separation is 12.1 Å,

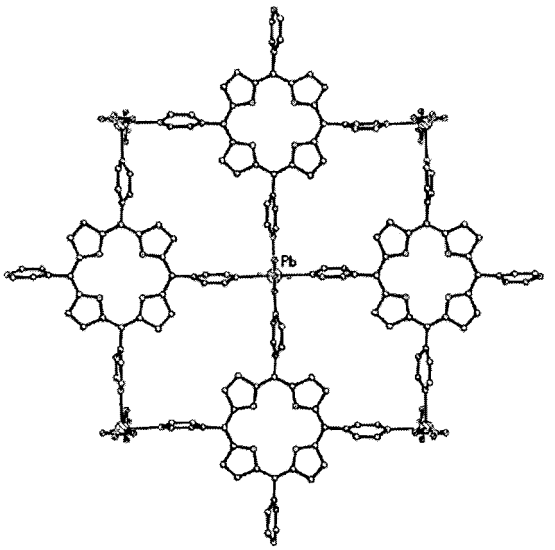

Fig. 1. Sheet structure of $H_2TpyP{\cdot}Pb(NO_3)_2$ layers in **1**.

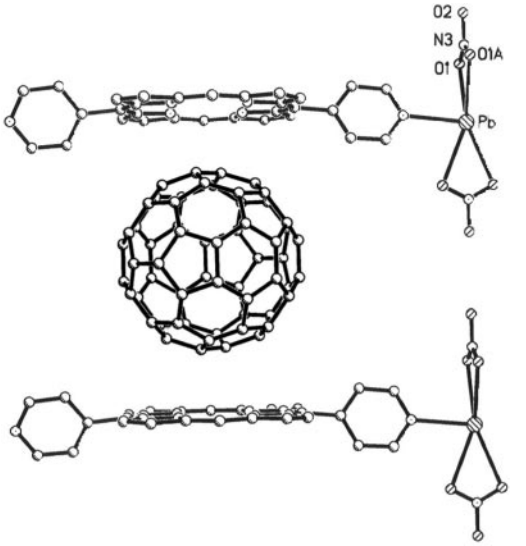

Fig. 3. Orientation of C_{60} over the center of the porphyrin in **1**.

accommodating the 10-Å van der Waals diameter of C_{60} and some solvent molecules. Without a fullerene present, the sandwiching of solvent molecules leads to an interlayer separation of 5.5 Å (15). As expected for a supramolecular association, there are no significant changes in the bond distances and angles of the components relative to those found in unassociated fullerene and porphyrin structures.

The other major difference concerns the vertical alignment of the porphyrin moieties. Compared with the offset (i.e., slipped) layers in the non-fullerene-containing species, the porphyrins in **1** show strict tetragonal register. We take this as important evidence that the porphyrin–fullerene supramolecular interaction is a structure-defining element.

The nature of the fullerene–porphyrin interaction is shown in Fig. 3. The fullerenes are precisely centered over the porphyrins. The C_2 axis of C_{60}, passing through the centers of diametrically opposed 6:6 ring juncture bonds, is aligned with a crystallographic fourfold axis. Crystallographic symmetry is maintained by rotational disorder with equal occupancy of two fullerene sites related by 90°. This orientation is proposed to arise from electrostatic considerations. The electron-rich 6:6 ring juncture is attracted to the protic region at the center of the porphyrin. The closest approach of a fullerene carbon atom to the mean plane of the 24-atom porphyrin core is 2.59 Å, the closest yet observed in a free-base porphyrin (24, 38). This may be the result of a compression, related to sandwiching the fullerenes between layers and minimizing crystal void space. The closest atom-to-atom contact between the components is a porphyrin N atom to fullerene C atom (at a 6:6 ring juncture) of 2.95 Å. Disordered TCE solvent molecules partially fill the voids in the lattice. The free volume in the structure for solvent is remarkably high: *ca.* 52%. This volume was estimated from the cavities left after the van der Waals surfaces were generated for the porphyrin/fullerene assembly. There are channels along the fourfold axis and the zigzag spaces perpendicular to the fourfold axis between the fullerenes.

A similar cocrystallization of $Pb(NO_3)_2$, H_2TpyP, and the larger, egg-shaped fullerene C_{70} also leads to crystalline intercalated material, **2**. To date, we have been unable to model the disordered C_{70} moiety in the x-ray structure. It sits on a fourfold symmetry site. However, it is clear from the partial solution that the overall structure is essentially the same as **1**. The fullerene has again brought the porphyrin layers into strict tetragonal register. The interlayer separation (12.5 Å) is slightly larger than that of C_{60}. Based on cocrystallization data (24) and complexation studies (27), we would expect the C_{70} moieties to be sandwiched between the porphyrins in side-on rather than end-on fashion. This arrangement maximizes van der Waals interactions, which, from molecular mechanics modeling (24), are the fundamental basis of the fullerene–porphyrin interaction. The data are consistent with this expectation but insufficiently accurate to confirm it.

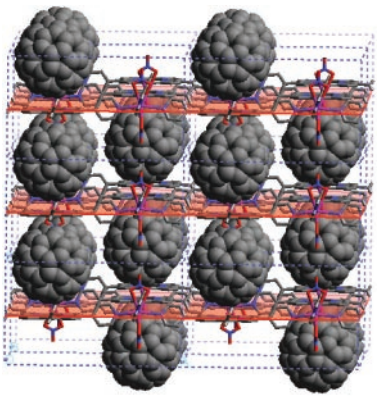

Fig. 2. Crystal packing in **1**, $C_{60}{\cdot}Pb(NO_3)_2{\cdot}(H_2TpyP){\cdot}1.5TCE$ (solvent molecules omitted for clarity).

Fullerene-Intercalated Ribbons. A related cocrystallization of HgI_2, H_2TpyP, and C_{70} yields a structure containing porphyrin ribbons rather than sheets. The porphyrin motif is very similar to that found in the non-fullerene-containing structures

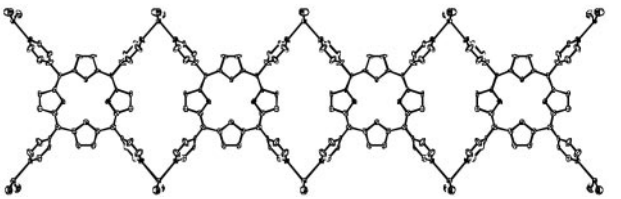

Fig. 4. Plan view of four units in the $H_2TpyP{\cdot}HgI_2$ ribbon structure in **3**.

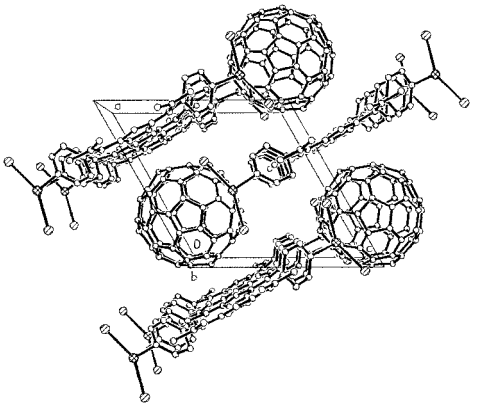

Fig. 5. Perspective view along the ribbon direction in $H_2TpyP{\cdot}HgI_2{\cdot}C_{70}$, **3**.

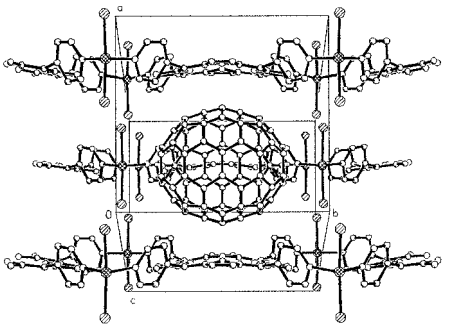

Fig. 6. Orientation of C_{70} over the porphyrin in **3**.

$(HgBr_2)_2(H_2TpyP){\cdot}2CHCl_3$ (**14**) and $(HgI_2)_2(H_2TpyP){\cdot}2TCE$ (**15**) (see Fig. 4).

As we have come to expect in fullerene structures, disorder in the C_{70} moiety thwarts a complete solution of single-crystal x-ray data. Nevertheless, a better solution than with **2** was possible, and the intercalated ribbon motif is clearly defined (see Fig. 5).

As in the sheet structures, the fullerene pries the ribbons *ca.* 12.5 Å apart. This spacing accommodates C_{70} in a side-on rather than end-on orientation with its fivefold axis parallel to the mean porphyrin plane (see Fig. 6).

With its band of hexagonal rings, the equatorial region of C_{70} is flatter than C_{60}-like polar regions. This is the expected result of maximizing van der Waals contact. It is observed in the discrete supramolecular chemistry of jaws porphyrin (27, 28) and cocrystallate structures (24, 39).

C_{70} also brings the porphyrins into perpendicular register between the ribbons. Indeed, in all three structures the fullerene is seen to shift the porphyrins from offset arrays into strictly vertical stacking relationships, without disturbing the structure within the layers or ribbons. This supports the idea that fullerene/porphyrin supramolecular recognition, not fullerene size, is controlling the structure. The solvent space in the ribbon structure is less than in the sheet structure: 30% compared with 52%.

Conclusions

The attraction of a fullerene to a porphyrin represents an additional supramolecular recognition element to engineer metal-organic frameworks and supramolecular solids. Past work has relied almost exclusively on hydrogen bonding or coordinate bonding to construct the scaffolding of framework structures. It should be possible to fine-tune the application with metals in the porphyrins because most metalloporphyrins bind to fullerenes about as well as do free-base porphyrins (28, 40).

Although the fullerene–porphyrin interaction is structure defining, it is clearly subservient to the stronger coordinate bonding to Pb or Hg that dictates the one-dimensional ribbon or two-dimensional sheet structures of the porphyrin arrays. Fullerene–fullerene interactions are seen in some fullerene–porphyrin crystal structures (24, 28) but they are weaker than fullerene–porphyrin interactions. True crystal engineering is a long way off (6), but the present work indicates a hierarchy of structure-defining elements that contributes a useful degree of design predictability to fullerene–porphyrin structure assembly. We anticipate the present molecular design principles will be most useful in the manipulation of photophysical properties, in adjusting charge transfer in molecular magnets and molecular conductors, and in the creation of new porous metal-organic frameworks. The electronic and infrared spectra of these materials reflect a simple summation of components, so ground state perturbation is weak. However, excited state interactions can be expected. Further work will be needed to understand how to exploit the weak interactions that must be present in the contiguous chromophores.

A present limitation of porphyrin framework structures as zeolite-like materials is their fragility toward loss of occluded solvent (13, 16). Typically, they collapse irreversibly upon total removal of solvent molecules. Preliminary experiments with **1** suggest that the fullerene pillars may ameliorate this problem somewhat but fall short of solving it. As judged by thermogravimetric analysis and elemental composition with SEM-EDX, approximately 80% of the solvent can be gradually removed by heating to 250°C under vacuum for 2 days. The powder x-ray diffraction pattern changes as a result of this treatment but there is no significant diminution of crystallinity. Complete removal of solvent above 300°C eventually leads to amorphous material that does not regain an XRD pattern upon exposure to TCE solvent vapor. We expect that more robust fullerene-pillared materials can be prepared if interporphyrin metal linkages stronger than Pb or Hg are used.

We thank Prof. G. M. Sheldrick for generous assistance in solving the x-ray crystal structure of **1**. This work was supported by the National Institutes of Health (GM 23851) and the Marsden Fund of The Royal Society of New Zealand (00-UOA-030).

1. Desiraju, G. R. (1995) *Angew. Chem. Int. Ed. Engl.* **34,** 2311–2327.
2. Aoyama, Y. (1998) *Top. Curr. Chem.* **198,** 131–161.
3. Zaworotko, M. J. (2000) *Angew. Chem. Int. Ed.* **39,** 3052–3054.
4. Dunitz, J. D. (1996) *Perspect. Supramol. Chem.* **2,** 1–30.
5. MacGillivray, L. R. & Atwood, J. L. (1999) *Angew. Chem. Int. Ed.* **38,** 1018–1033.
6. Robson, R. (2000) *J. Chem. Soc. Dalton Trans.* 3735–3744.
7. Bryn, M. P., Curtis, C. J., Goldberg, I., Hsiou, Y., Khan, S. I., Sawin, P. A., Terzis, A. & Strouse, C. E. (1991) *J. Am. Chem. Soc.* **113,** 6549–6557.
8. Kosal, M. E. & Suslick, K. S. (2000) *J. Solid State Chem.* **152,** 87–98.
9. Abrahams, B. F., Hoskins, B. F., Michail, D. M. & Robson, R. (1994) *Nature (London)* **369,** 727–729.
10. Drain, C. M. & Lehn, J.-M. (1994) *J. Chem. Soc. Chem. Commun.,* 2313–2315.
11. Drain, C. M., Nifiatus, F., Vasenko, A. & Batteas, J. D. (1998) *Angew. Chem. Int. Ed.* **37,** 2344–2347.
12. Kumar, R. K., Balasubramanian, S. & Goldberg, I. (1998) *Inorg. Chem.* **37,** 541–552.
13. Goldberg, I. (2000) *Chem. Eur. J.* **6,** 3863–3870.
14. Pan, L., Noll, B. C. & Wang, X. (1999) *Chem. Commun.,* 157–158.
15. Sharma, C. V. K., Broker, G. A., Huddleston, J. G., Baldwin, J. W., Metzger, R. M. & Rogers, R. D. (1999) *J. Am. Chem. Soc.* **121,** 1137–1144.
16. Lin, K.-J. (1999) *Angew. Chem. Int. Ed.* **38,** 2730–2732.
17. Hagrman, D., Hagrman, P. J. & Zubieta, J. (1999) *Angew. Chem. Int. Ed.* **38,** 3165–3168.
18. Yaghi, O. M., Li, H., Davis, C., Richardson, D. & Groy, T. L. (1998) *Acc. Chem. Res.* **31,** 474–484.

19. Gardner, G. B., Venkataraman, D., Moore, J. S. & Lee, S. (1995) *Nature (London)* **374,** 792–795.
20. Aoyama, Y., Endo, K., Kobayashi, K. & Masuda, H. (1995) *Supramol. Chem.* **4,** 229–241.
21. Kepert, C. J. & Rosseinsky, M. J. (1999) *Chem. Commun.,* 375–376.
22. Chen, B., Eddaoudi, M., Hyde, S. T., O'Keeffe, M. & Yaghi, O. M. (2001) *Science* **291,** 1021–1023.
23. Sun, Y., Drovetskaya, T., Bolskar, R. D., Bau, R., Boyd, P. D. W. & Reed, C. A. (1997) *J. Org. Chem.* **62,** 3642–3649.
24. Boyd, P. D. W., Hodgson, M. C., Chaker, L., Rickard, C. E. F., Oliver, A. G., Brothers, P. J., Bolskar, R., Tham, F. S. & Reed, C. A. (1999) *J. Am. Chem. Soc.* **121,** 10487–10495.
25. Olmstead, M. M., Costa, D. A., Maitra, K., Noll, B. C., Phillips, S. L., Van Calcar, P. M. & Balch, A. L. (1999) *J. Am. Chem. Soc.* **121,** 7090–7097.
26. Tashiro, K., Aida, T., Zheng, J.-Y., Kinbara, K., Saigo, K., Sakamoto, S. & Yamaguchi, K. (1999) *J. Am. Chem. Soc.* **121,** 9477–9478.
27. Sun, D., Tham, F. S., Reed, C. A., Chaker, L., Burgess, M. & Boyd, P. D. W. (2000) *J. Am. Chem. Soc.* **122,** 10704–10705.
28. Sun, D., Tham, F. S., Reed, C. A., Chaker, L. & Boyd, P. D. W. (2002) *J. Am. Chem. Soc.* **124,** in press.
29. Guldi, D. M. (2000) *Chem. Commun.,* 321–327.
30. Segura, J. L. & Martin, N. (2000) *Chem. Soc. Rev.* **29,** 13–25.
31. Armaroli, N., Marconi, G., Echegoyen, L., Bourgeois, J.-P. & Diederich, F. (2000) *Chem. Eur. J.* **6,** 1629–1645.
32. Kahn, O. (1993) *Molecular Magnetism* (VCH, New York).
33. Eichhorn, D. M., Yang, S., Jarrell, W., Baumann, T. F., Beall, L. S., White, A. J. P., Williams, D. J., Barrett, A. G. M. & Hoffman, B. M. (1995) *J. Chem. Soc. Chem. Commun.,* 1703–1704.
34. Konarev, D. V. & Lyubovskaya, R. N. (1999) *Uspekhi Khimii (Russ. Chem. Rev.)* **68,** 23–44 (19–38).
35. Bruker (1997–1998) SMART *Software Reference Manual* (Bruker Analytical X-Ray System, Madison, WI), Version 5.054.
36. Bruker (1997–1998) SAINTPLUS *Software Reference Manual* (Bruker Analytical X-Ray System, Madison, WI), Version 5.02.
37. Bruker (1997–1998) SHELXTL *Software Reference Manual* (Bruker Analytical X-Ray System, Madison, WI), Version 5.1.
38. Evans, D. R., Fackler, N. L. P., Xie, Z., Rickard, C. E. F., Boyd, P. D. W. & Reed, C. A. (1999) *J. Am. Chem. Soc.* **121,** 8466–8474.
39. Konarev, D. V., Neretin, I. S., Slovokhotov, Y. L., Yudanova, E. I., Drichko, N. V., Shul'ga, Y. M., Tarasov, B. P., Gumanov, K. L., Batsanov, A. S., Howard, J. A. K. & Lyubovskaya, R. N. (2001) *Chem. Eur. J.* **7,** 2605–2616.
40. Zheng, J.-Y., Tashiro, K., Hirabayashi, Y., Kinbara, K., Saigo, K., Aida, T., Sakamoto, S. & Yamaguchi, K. (2001) *Angew. Chem. Int. Ed.* **40,** 1858–1861.